

THE PADME EXPERIMENT

F. Bossi, E. Capitolo (Tec.), C. Capocchia (Tec.), S. Ceravolo (Tec.), R. De Sangro,
C. Di Giulio, D. Domenici, G. Finocchiaro, L.G. Foggetta, M. Garattini (AdR),
A. Ghigo, P. Gianotti (Resp.), V. Kozhuharov (Ass.), M. Mancini (Ass.),
I. Sarra, T. Spadaro, E. Spiriti, C. Taruggi (AdR), E. Vilucchi

1 Introduction

One of the most intriguing mysteries in physics today, is that the matter seen in the universe accounts only for about 5% of the observed gravity. This has triggered the idea that enormous amounts of invisible dark matter should be present.

Among the different theoretical models that try to define what dark matter could be, there are those postulating the existence of a “Hidden Sector” populated by new particles living independently from those of the Standard Model (SM). The connection within these two worlds is theoretically realized by a low-mass spin-1 particle, indicated with the symbol A' , that would manifest as a gauge coupling of electroweak strength to dark matter, and a much smaller coupling to the SM hypercharge ¹⁾. This Dark Photon (DP) could be the portal connecting ordinary and the dark world.

The PADME experiment aims to search for signals of such a DP studying the reaction:

$$e^+e^- \rightarrow \gamma A' \tag{1}$$

using the positron beam of the LNF LINAC and identifying the A' as a missing mass signal.

PADME (Positron Annihilation into Dark Matter Experiment) is an international collaboration that in 2022 counted about 30 scientists from LNF, the INFN sections of Roma1, Torino and Lecce, the Sapienza University of Rome (IT), the Salento University (IT), the Torino Politecnico (IT), the Sofia University (BG), the Princeton University (USA).

The apparatus was built, installed and commissioned with the beam from October 2018 to February 2019 (Run-I). In 2020 a new data acquisition period (from July to December 2020) took place. The first part was dedicated to beam tuning and detector calibration, while from September $\sim 5 \times 10^{12}$ positrons-on-target (POT) were recorded to start addressing the main physics goal (Run-II).

The PADME detector can actually study other scientific issues, namely the production of any dark particle in the in-flight annihilation of positrons on the electrons of the target either associated with an ordinary photon $e^+e^- \rightarrow \gamma X$, or resonantly $e^+e^- \rightarrow X$. This feature, combined with the possibility to change easily and precisely the beam energy, turned out ideal to study the existence of a new particle named X_{17} . This state was introduced to explain an anomalous behaviour observed by a nuclear physics experiment performed at the ATOMKI institute of Debrecem in Hungary. The experiment was studying the de-excitation of some high energy nuclear states (^8Be , ^4He , ^{12}C) via Internal Pair Creation. In the angular distribution of the measured e^+e^- pairs, a bump appeared and the most plausible explanation of such behaviour is to admit that the decay of the excited state proceeds through the creation of an unstable particle of mass $\sim 17 \text{ MeV}$ ²⁾. If the existence of this state will be confirmed, it will represent the first evidence of dark matter produced at accelerator experiments.

2 The PADME experiment

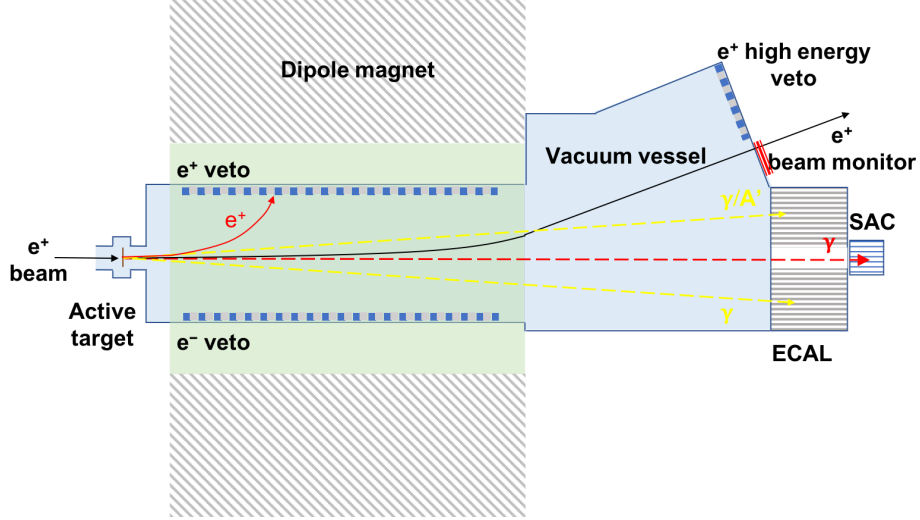


Figure 1: *The layout of the PADME experiment. From left to right: the active target, the positron/electron vetoes inside the magnetic field, the high energy e^+ veto near the non-interacting beam exit, the e.m. calorimeters (ECal, SAC), the solid state beam monitor detector.*

The main goal of the PADME experiment is to search for DPs produced in the annihilation process of the positron beam of the LNF LINAC with the electrons of a thin, low Z target and then identified using a missing mass technique ³⁾.

Figure 1 shows a scheme of the apparatus whose basic elements are:

- a low divergence positron beam, impinging on a thin, diamond active target, capable of monitoring the beam spot and intensity;
- a vacuum chamber to avoid spurious particle interactions;
- a magnet to deflect the non-interacting positrons, and with the additional task of allowing the measurement of the momentum of the interacting positrons, thus contributing to the rejection of the Bremsstrahlung background;
- a finely-segmented, high-resolution e.m. calorimeter (ECal), with the main purpose to detect the single SM photon of reaction 1. ECal has in the center, a square hole to allow high frequency Bremsstrahlung photons to pass through;

Since the processes that mainly take place in the beam-target interaction are Bremsstrahlung and $e^+e^- \rightarrow \gamma\gamma(\gamma)$, to cut out these background events, two extra components are crucial:

- a fast Small Angle Calorimeter (SAC), placed behind the central hole of ECal. This is used to detect and veto background photons (mainly from Bremsstrahlung);
- three series of plastic scintillator bars located inside the vacuum chamber, two within the dipole magnet gap (Pveto and Eveto), and the third one on the beam exit (HEPveto). Their purpose is to veto charged particles produced in the interaction.

To allow a more accurate monitoring of the beam, in the target region are installed two planes of silicon pixel detectors placed up and down stream the active diamond target. Each plane consists of two MIMOSA 28 Ultimate chips, developed for the upgrade of the STAR vertex detector ⁴⁾. These devices integrate a Monolithic Active Pixel Sensor (MAPS) with a fast binary readout. Each sensor consists of a matrix of 928×960 pixels of $20.7 \mu\text{m}$ side with a thickness of $50 \mu\text{m}$. For the STAR experiment the chips, that dissipate $150 \text{ mW}/\text{cm}^2$, operate in air without cooling. For PADME, the detectors have been placed in vacuum and a modified PCB, providing cooling, has been developed by the LNF electronic service.

The MIMOSA detector cannot stay on the beam line during the data taking, therefore an extra monitoring device is placed out of the vacuum on the positron beam exit trajectory. This is an array (6×2) of Timepix3 chips ⁵⁾ able to record either the time-of-arrival (ToA) and the energy of the incident particles providing excellent energy and time resolutions. Each silicon chip (designed in 130 nm CMOS technology) contains 256×256 pixels ($55 \times 55 \mu\text{m}^2$) ⁶⁾. The individual sensors in the Timepix3 beam monitor can operate in two modes: in frame mode, which integrates the ToA and ToT data over a time interval and provides the output as a 256×256 pixels picture frame; or in data-driven mode. In this second mode the data from individual pixels are provided as a stream, and it is up to the application that consume this data to treat them appropriately.

3 Activity of the PADME Group in 2022

Year 2022 has been mainly devoted to the analysis of data collected in Run-II and to the preparation of Run-III dedicated to the X_{17} search.

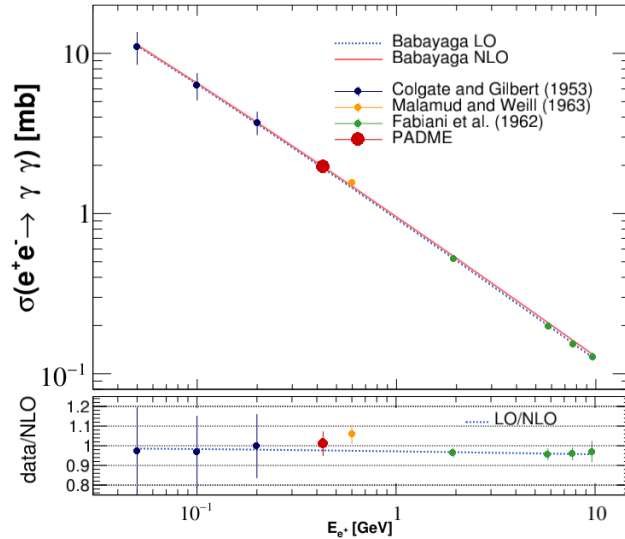


Figure 2: *Theory predictions, at the leading order and next-to-leading order approximation, for the positron annihilation cross-section in flight as a function of the positron energy. The PADME measurement is superimposed along with earlier measurements. Data to theory ratios are shown in the bottom pad.* ⁷⁾

The evaluation of the missing mass of single photon final states, is the last step of a long

sequence of operations necessary to tune at best the detector response. Two photon events can be used to assess single-photon reconstruction efficiency in PADME that is crucial for the DP analysis. Then, to test completely the behaviour of the PADME detector, it has been performed the measurement of the absolute cross-section of the process $e^+ + e^- \rightarrow \gamma\gamma$ with a precision of 5% and compared it with the expectation of SM calculations. The measurement has been performed on a subset of the PADME Run-II data of 4×10^{11} POT collected with a positron energy of 432.5 MeV, corresponding to $\sqrt{s} = 21$ MeV. The result is shown in Fig. 2 together with previous measurements and theoretical predictions.

The physics potential of the PADME experiment extends beyond DP search. Profiting by the unique possibility of having positrons in the energy range 270-300 MeV, PADME is in the ideal position to produce the X_{17} state in a resonant mode and subsequently detect it via its decay to an e^+e^- pair. The PADME Run-III (from October to December 2022) was then conceived to perform an energy scan of the X_{17} mass region. In the peculiar situation of knowing the mass of the particle to the level of few hundreds KeV, the particle can be identified counting the number of e^+e^- pairs produced at different beam energies and compare it to what is expected from the SM. Phenomenological studies have been performed to establish the PADME sensitivity based on two different scenarios for the beam energy resolution and the total number of collected POT per point:

- *conservative*, 12 points summing up to 2×10^{11} total PoT, with a 0.5% beam energy spread, in the energy range 265–297 MeV;
- *aggressive*, 14 points summing up to 4×10^{11} total PoT, with 0.25% beam energy spread, in the narrower energy range 273–291 MeV;

Figure 3 shows the projected 90% C.L. sensitivity of PADME Run-III on the couplings of a X_{17} boson for the *conservative* (solid orange line) and *aggressive* (dashed orange line) option. Two different hypotheses on the X_{17} quantum numbers are considered: 1^{--} (left) and 0^{-+} (right). The

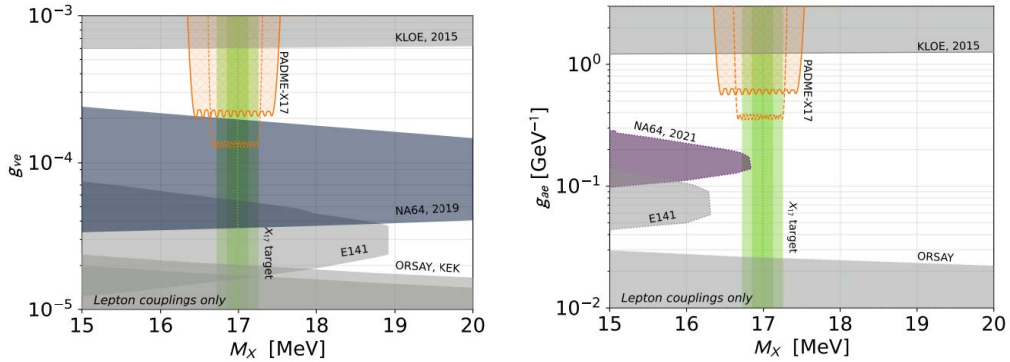


Figure 3: *left: PADME expected sensitivity to a vector X_{17} . right: PADME expected sensitivity to a pseudo-scalar X_{17} ⁸⁾. Two different energy scan hypotheses have been considered (see text for more details). Different grey areas represent the excluded regions for the couplings coming from other experiment.*

main background to the $X_{17} \rightarrow e^+e^-$ signal is the elastic (Bhabha) electron-positron scattering. While the t -channel is peaked at high energies for the scattered positron, the s -channel has the same signal kinematics. In addition, two clusters from $\gamma\gamma$ events have to be rejected. Since the

PADME veto spectrometer cannot be used to constrain e^+e^- vertices not originating from the target, it has been decided to identify the decays of the X_{17} using the ECal. Thus, to allow low-momentum charged particles to reach the calorimeter, the magnetic field has been switched off. In order to disentangle e^+e^- from photons an additional detector (the electron tagger, ETag) has been realized and installed in front of ECal. The ETag is made of 5 mm thick scintillator slabs, each read out by 4 SiPMs identical to those of the Veto systems. The vertical segmentation of the detector (4 cm) allows to have a sustainable rate while covering the fiducial region of the calorimeter with a reasonable number of channels (Fig. 4).



Figure 4: *The PADME lepton tagger detector (ETag) being assembled in front of the BGO calorimeter (ECal).*

The high particle multiplicity ($\sim 100 e^+/ns$) provided by the LINAC results in multiple pulses in the individual detector elements of the PADME setup. The long decay time of the BGO, about 300 ns, makes double pulses separation necessary, but a difficult task. A machine learning method based on convolutional neural networks was developed in 2022 aiming both at the identification and at the reconstruction of the properties of overlapping pulses in the ECal channels. The topology of the neural network mimics an autoencoder but the desired output are the deconvoluted moments of particle energy deposits in the detecting elements. The initial results obtained applying this algorithm are promising. Time resolutions of ~ 500 ps for ECal double pulses were reached.

A key detector of the PADME experiment is the Timepix3 beam monitor. This detector consists of an array of sensors (6×2) able to perform data acquisition keeping the pixels sensitive at all times when in operation. Up to Run-III the detector was readout independently from the main PADME DAQ system using the data acquisition software provided by the vendor company (ADVACAM). Unfortunately, this program showed problematic synchronization issues of the individual chips that severely limited the the ability to acquire data for times longer than a few minutes. Thus a complete new software to acquire and analyze the Timepix3 data was developed, allowing to operate the sensors in both frame and data-driven mode. The new software resolved most of the operational problems by implementing better sensor fault recovery algorithms and an improved communication protocol. This allow to regularly use Timepix3 detector during the whole Run-III to monitor the positron beam characteristics (see fig 5).

4 List of Conference Talks presented by LNF Speakers in Year 2022

Here below, it is the list of conference presentations given by LNF PADME members:



Figure 5: *Beam spot picture resulting from ToT measurements performed with Timepix3 detector.*

1. V. Kozhuharov, “The PADME experiment at LNF-INFN”, invited talk at the *11th International Conference of the Balkan Physical Union (BPU11)*, Belgrade, 28 Aug. – 1 Sep. 2022.
2. P. Gianotti, “The study of the X17 anomaly with the PADME experiment”, talk at the *The 28th International Nuclear Physics Conference (INPC 2022)*, Cape Town, 11 – 16 Sep. 2022.
3. T. Spadaro, “Ricerche di materia oscura nell’esperimento PADME”, invited talk at the *Convegno Nazionale Società Italiana di Fisica*, Milano, 12 – 16 Sep. 2022.
4. D. Domenici, “Dark sector studies with the PADME experiment”, talk at the *Physics of fundamental Symmetries and Interactions (PSI2022)*, Villingen, 16 – 21 Oct. 2022.

For the complete list of presentations to conferences given by the PADME collaborators, refer to <http://padme.lnf.infn.it/talks/>.

5 List of Publications by LNF Authors in Year 2022

Here below, it is the list of papers published by PADME LNF members in 2022:

1. P. Albicocco *et al.*, “Commissioning of the PADME experiment with a positron beam”, *JINST* 17 (2022) 08, P08032, ArXiv:2205.03430 [physics.ins-det]
2. F. Bossi *et al.*, “The PADME beam line Monte Carlo simulation”, *JHEP* 09 (2022) 233 ArXiv:2204.05616 [hep-ex]
3. P. Gianotti, “The PADME scientific program”, *PoS PANIC2021* (2022) 043

The complete list of papers published by the PADME collaboration in 2019 can be find here <http://padme.lnf.infn.it/papers/>.

References

1. B. Holdom, *Phys. Lett. B* 166, 196 (1986).
M. Pospelov, *Phys. Rev. D* 80, 095002 (2009).

2. A. J. Krasznahorkay *et al.*, Phys. Rev. Lett. 116 (2016) 042501.
A. J. Krasznahorkay *et al.*, Phys. Rev. C 104 (2021) 044003.
A. J. Krasznahorkay *et al.*, Phys.Rev.C 106 (2022) L061601.
3. M. Raggi and V. Kozhuharov, Rivista del Nuovo Cimento 38 no. 10 (2015).
DOI 10.1393/ncr/i2015-10117-9.
4. I. Valin *et al.*, JINST 7, C01102 (2012).
5. T. Poikela *et al.*, JINST 9, C05013 (2014).
6. ADVACAM s.r.o., U Pergamenky 12, 17000 Praha 7, Czech Republic, (<https://advacam.com>).
7. F. Bossi *et al.*, Phys. Rev. D 107 (2023) 012008.
8. L. Darmé, M. Mancini, E. Nardi and M. Raggi, Phys. Rev. D 106 no. 11 (2022) 115036.